Mechanical characterization and modelling of Ultra High Performance Fiber Reinforced Concrete

Sara Bascì, Matteo Colombo, Giulio Zani

Dept. Of Civil and Environmental Eng.
Politecnico di Milano
Piazza Leonardo da Vinci 32, Milan (20133), Italy

Abstract
In the last two decades the use of Ultra High Performance Fiber Reinforced Concrete (UHPFRC) for the construction of structural and non-structural elements has increased, but there is still a strong need to establish a complete method for its mechanical characterization, especially of its tensile behavior. In this paper, a mechanical investigation carried out on four UHPFRC specimens with a fiber volume fraction of 3.3% is presented. The fiber content resulted to be sufficient to cause strain hardening behavior, characterized by a multicracking phase. The tensile constitutive law provided by Model Code 2010 for the inverse analysis from bending tests is hereby discussed. In particular, the size of the multicrack diffusion zone is investigated with vision-based measurement tools and used as a characteristic length.

1 Introduction

UHPFRC is the object of numerous studies and its use is becoming increasingly widespread. Thanks to its mix design, it is able to achieve high aesthetic and mechanical requirements, but its mechanical characterization, especially in terms of tensile behavior, is still much debated. Direct tensile testing might be an appropriate method to directly derive the tensile strength of the material since it does not require inverse analysis [1]. On the other hand, direct tensile tests are difficult to perform due to the complexity of the setup and its sensitivity to various factor (imperfections in the specimen, stress concentrations at its attachment points, etc.), therefore could not produce completely reliable results [2]. In answer to this question, several codes propose to define the tensile behavior by means of bending tests and subsequent inverse analysis. As a matter of fact, the current Fiber Reinforced Concrete standard (Model Code 2010 [3]) proposes a simplified approach to find the stress-strain relationship in tension. In order to use the constitutive law in the Finite Element Model (FEM) and make it mesh independent, it is possible to perform a fracture energy regularization by dividing the crack opening displacement by the mesh size. However, this procedure leads to an overestimation of the tensile behavior in hardening materials which are characterized by a multicracking phase that prevents the crack from localizing in a single section [4]. This paper takes part of this framework by presenting an experimental campaign on notched beams tested with the three-point bending scheme (3PB). The mechanical response of the material and the inverse analysis of the results are discussed. Some considerations on the parameters for the definition of the constitutive law according to the Model Code 2010 will be presented.

Fig. 1 Straight high carbon steel fibers (left); specimens just after casting (right).

2 Materials

The UHPFRC used to cast the specimens is characterized by a mix design consisting of a premixed concrete in which only water, superplasticizer and steel fibers have to be added separately. The average cubic compressive strength ($f_{c,cube,av}$), obtained from the laboratory tests, was equal to 153.2 MPa.

Straight high carbon steel fibers with a length (l_f) of 13 mm, a diameter (d_f) of 0.16 mm and thus an aspect ratio (l_f/d_f) of 80 were used (Fig. 1 (left)). The amount of fibers used was 236.2 kg/m^3 which corresponds to 3.3% in terms of volume. The mix design is summarized in Table 1.

Table 1 UHPFRC mix design.

Component	Dosage [kg/m^3]
premix	2105.3
water	129.5
superplasticizer	37.9
steel fibers	263.2

3 Experimental investigation

Four 150 x 150 x 600 mm notched beams were casted (Fig. 1 (right)) and tested by 3PB following EN 14651 [5] standard procedures. The tests were carried out at the laboratory of the Politecnico di Milano (Campus Lecco) with a hydrodynamic press characterized by a load capacity of 150 kN. All the tests were performed in crack-opening control with a rate of 0.05 mm/min until a crack opening of 0.1 mm is achieved and then increased to 0.2 mm/min as required by standard EN 14651. To provide measurement of the crack mouth opening displacement (CMOD) and of the crack tip opening displacement (CTOD), each specimen was instrumented, respectively, with a clip gauge located astride the notch and a linear variable displacement transducer (LVDT) with a gauge length of 50 mm positioned to be aligned and centered relative to the innermost edge of the notch (Fig. 2 (left)).

In standard softening materials, the expected response is crack propagation only at the notch. In hardening materials, such as UHPFRC, the crack may also occur outside the notched section. These phenomena are difficult to identify with normal instrumentation applied to specimens, but they may have an important contribution in identifying the direct tensile response of the material. For this reason, an alternative measurement method was chosen and applied to the specimen coded as 3PB-4. (Fig. 2 (right)). The technique used is Digital Image Correlation (DIC), which enables the non-contact full-field measure of geometry, displacement and strain [6] of materials and structures and is based on the correlation of two grey-scale images taken at different time instants, before and after deformation. To prepare the DIC setup the first step was to prepare the Area of Interest (AoI) of the specimen with a stochastic pattern. The surface was painted uniformly with a white spry can and once dry was sprayed with a damaged black one. A speckle pattern of black dots ranging in size from approximately 0.2 to 3.5 mm were obtained and the coverage factor, i.e. the percentage of black dots on the white background, was calculated as around 13%. To check the flatness of the acquired images and to easily convert pixels to millimeters and vice versa, two targets with four crosses placed between them at a known distance of 10 mm were applied at the two opposite vertices of the AoI. A bright spotlight was placed pointing at the surface of the specimen to provide proper illumination to address the requirement for high quality images and therefore sufficient exposure and high contrast. Afterwards a 24 Megapixel camera with a focal length of 50 mm was positioned 30.6 cm from the specimen to cover an AoI of 200 x 150 mm (Fig. 3). Finally, an image acquisition rate of 3 seconds was set. A higher frequency was not chosen to lighten the subsequent data processing, which would otherwise have taken a considerable amount of time without adding information to the processed data.

4 Results and discussion

4.1 Mechanical response

Fig. 4 shows the experimental results in terms of nominal stress versus CMOD of the four specimens tested at 3PB and Table 2 presents the following data: flexural tensile strength ($f_{ct,fl}$); residual strength

for serviceability conditions at CMOD = 0.5 mm (f_{R1}); residual strength for ultimate conditions at CMOD = 2.5 mm (f_{R3}); for each parameter even mean value, coefficient of variation (CoV) and characteristic value according to log-normal distribution are presented. Following the guidelines provided by Model Code 2010 about the FRC classification, the material investigated results in the class 19b.

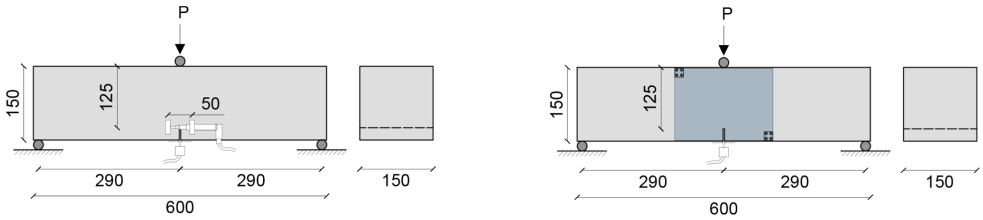

Fig. 2 Specimens geometry and 3PB setup (left); AoI for DIC (right).

Fig. 3 a) Scheme of the focal length and the distance needed between the camera and the specimen to obtain the required AoI dimension; b) image captured by the camera, it is possible to observe the stochastic pattern; c) setup on test specimen 3PB-4, the AoI is highlighted by blue rectangle.

Table 2 Experimental results of 3PB tests.

Specimen code	$f_{ct,fl}$ [MPa]	f_{R1} [MPa]	f_{R3} [MPa]
3PB-1	11.85	18.09	14.73
3PB-2	12.41	22.73	17.58
3PB-3	12.64	19.77	12.12
3PB-4	10.72	18.49	13.55
$f_{i,mean}$ [MPa]	11.9	19.77	14.5
Cov [%]	0.07	0.11	0.16
$f_{i,k}$ [MPa]	9.79	15.02	9.51

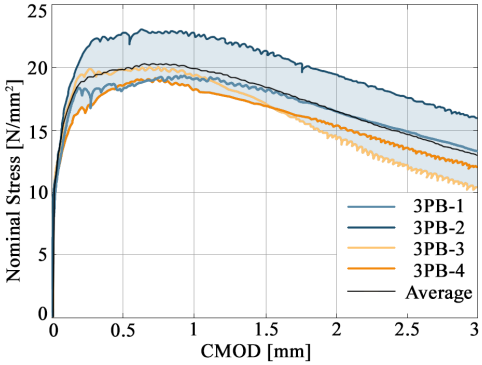

Fig. 4 Nominal Stress vs. CMOD for the four specimens, average curve and results scatter.

4.2 Vision-based measurements

The images acquired during the test were processed with Matlab-based DIC code - version 4 developed by E. M. C. Jones [7]. Briefly, the images were correlated, the optimal subset size for the correlation of full-images was determined, the displacements were smoothed with the Gaussian distribution of weight and finally strains were calculated using a 16-node, bi-cubic finite element interpolation scheme. The effective resolution of the images is 34 μm/pixel, which allows micro-displacements and therefore microcracks to be precisely investigated.

Fig. 6 represents the strain distribution over the AoI at the load steps, from a) to h), indicated on the stress versus CMOD curve of Fig. 5 (left). Point a) represents the crack initiation at the notch tip. In the phase from a) to c) a localization of the strain can be noticed. Starting from point d) a crack bifurcation is observable from the DIC images and in the following steps a clear multicracking pattern is visible although dominated by a wider central crack in correspondence of the notch.

As highlighted in Fig. 5 (right), corresponding to step h), the region characterized by the presence of microcracks has an extension of about 65 mm. It is worth noting that after point h) the large displacements achieved by the sample lead to a loss of image correlation processed with the adopted DIC software. Therefore, from that point on, it is no longer possible to obtain reliable results. In Fig. 5 (right) it is already possible to observe a partial loss of image correlation. This loss is represented by the white areas in correspondence of the main crack starting from the notch.

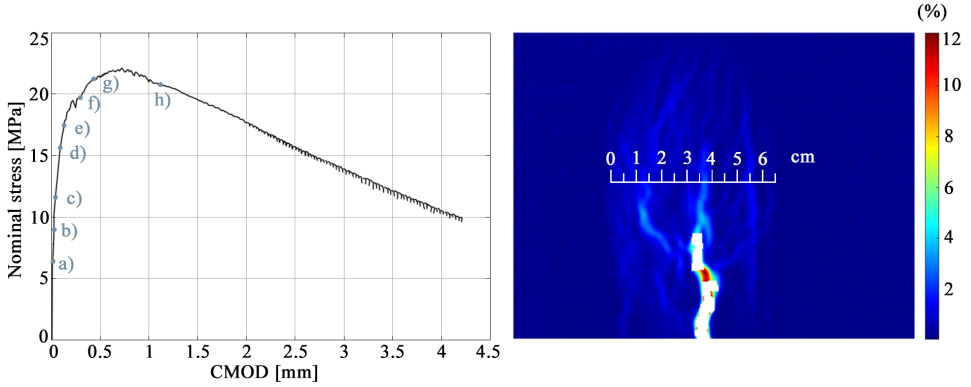

Fig. 5 Nominal stress vs. CMOD curve of 3PB-4 specimen. The letters from (a) to (h) correspond to the steps shown in the following Fig. (left); strains of step h) obtained by processing the images with the DIC software used. The width (equal to 65 mm) of the area characterized by the multicrack phenomenon is highlighted (right).

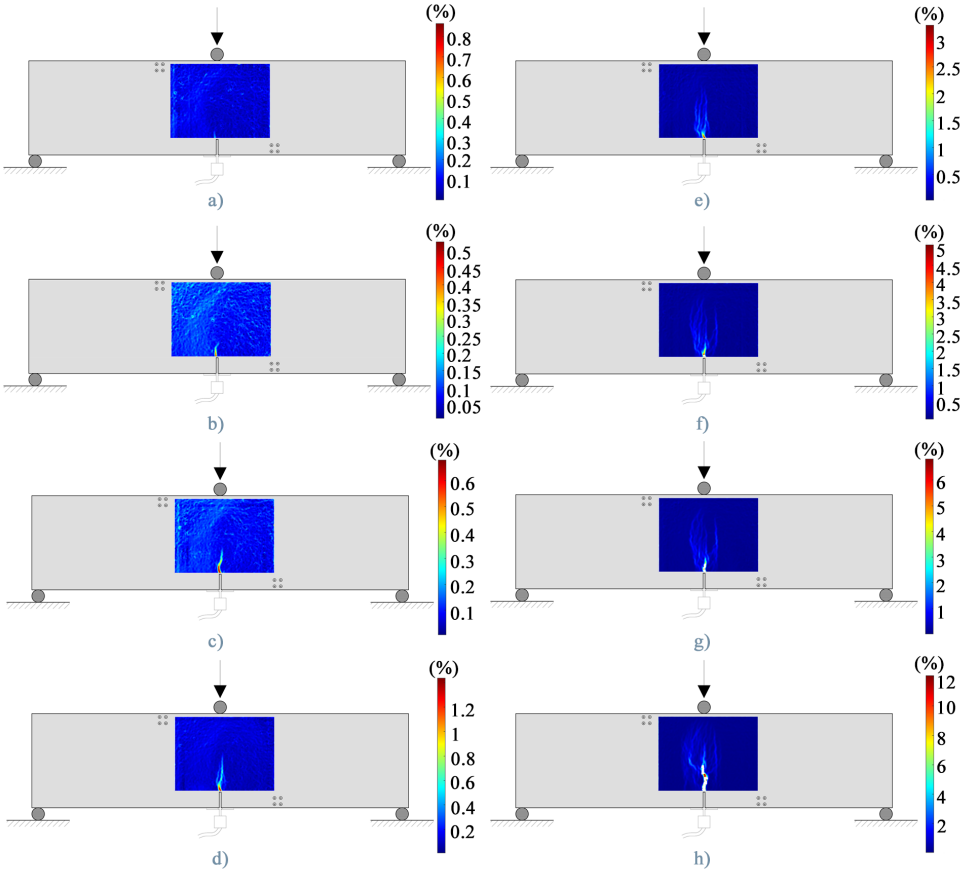

Fig. 6 Strains obtained from DIC in eight selected steps corresponding to the points highlighted in the curve in Fig. 5 (left).

4.3 Numerical modelling

A numerical investigation, aimed at discussing the uniaxial tensile constitutive law to be adopted for non-linear finite elements model in case of strain-hardening material, is here proposed with reference to the use of Concrete Damage Plasticity model implemented in Abaqus. Several uniaxial constitutive laws were adopted to model 3PB tests previously discussed. Notched beam is discretized using plane stress elements 4-node bilinear with reduced integration and hourglass control (CPS4R) and a regular quadrangular mesh with elements of side 2.5 mm (Fig. 8 (left)). The uniaxial tensile laws were assigned in terms of stress versus plastic strain relationships where the plastic strains were defined dividing the crack opening (w) by a characteristic length (l_{ch}). The adopted laws differ by the value of the l_{ch} and/or the shape of the constitutive law. In particular, the following cases were analyzed and summarized in Fig. 7 and Table 3:

A) use of the uniaxial tensile law proposed by Model Code 2010 assuming a l_{ch} equal to di element size (2.5 mm) as suggested by the traditional fracture energy regularization approach for concrete [8];

B) use of the uniaxial tensile law proposed by model Code 2010, but assuming for the strain related to f_{Fts}, a l_{ch} value equal to 65 mm which represents the size of the microcrack diffusion zone measured by DIC (Section 4.2). For the point corresponding to the ultimate residual strength (f_{Ftu}), since it is located on the softening branch of the tensile law, an l_{ch} equal to the element size was adopted;

C) use of a constitutive law similar to those proposed by Model Code 2010 but modified at point f_{Fts} according to [9] ($f_{Fts} = 0.37 \cdot f_{R1}$). The same l_{ch} of case B were applied;

D) a modified shape of the pre-peak branch was adopted considering pre-peak data deriving from the data available in the literature on similar material. In particular, the value of the axial tensile strength (f_{ct}, equal to 9 MPa), the corresponding strain (equal to 0.38%) and the value of the elastic modulus (E, equal to 45000 MPa) were selected. The post-peak law and the values of l_{ch} adopted are the same of case C.

The results of all the numerical investigations are captured with the average experimental curve in Fig. 8 (right) in terms of nominal stress versus CMOD. In Table 3 the total energy (computed as the area under the nominal stress versus CMOD curve up to CMOD = 3 mm) is reported for each model together with its percentage difference with respect to the experimental one. As can be seen, the nominal stress versus CMOD curve of case A, despite the reliable prediction of the total energy, does not capture the shape of the pre-peak and overestimates the tensile properties by showing a hardening behavior at least up to a CMOD of 3 mm. Case B, having considered the measured dimension of the multicracking region, continue to over-estimating the performances of the material (even in terms of total energy) but starts to activate a softening branch even if the peak position (both in terms of stress and CMOD) is not reliable. Case C provides a good approximation of the peak stress but leads to an under-estimation of the stable propagation phase and an over-estimation of the fiber pull-out phase. Finally, case D succeeds in capturing the behavior at low crack opening values and in predicting the peak (both stress and CMOD) with a minimum over-estimation of the total energy that is mainly concentrated in the final branch with large CMOD (CMOD > 1.5 mm). This is probably due to the simplification of the model proposed by Model Code 2010 which determines the stress value corresponding to CMOD = 2.5 mm from equilibrium with the assumption that the compressive stress resultant is applied on the extrados chord and that the tensile behavior is rigid-linear. Looking at the plastic strain distribution shown in Fig. 8 (left) it is possible to observe that they are mainly concentrated in the ligament section.

Table 3 Cases analyzed and variables considered to reconstruct the constitutive tensile relation to be used in the analytical model (experimental total energy equal to 51,3 N/mm).

Model	E [MPa]	f_{ct} (or $\overline{f_{ct}}$) [MPa]	f_{Fts} [MPa]	f_{Ftu} [MPa]	ε_p (or $\overline{\varepsilon_p}$) [%]	l_{ch}^{SLS} [mm]	l_{ch}^{USL} [mm]	Total energy [N/mm]
A	50300	5.6	8.9	3.3	0.015	2.5	2.5	54.3 (+5.8%)
B	50300	5.6	8.9	3.3	0.015	65	2.5	64.1 (+24.7%)
C	50300	5.6	7.3	3.3	0.015	65	2.5	55.7 (+8.5%)
D	45000	9	7.3	3.3	0.38	65	2.5	53.3 (+3.8%)

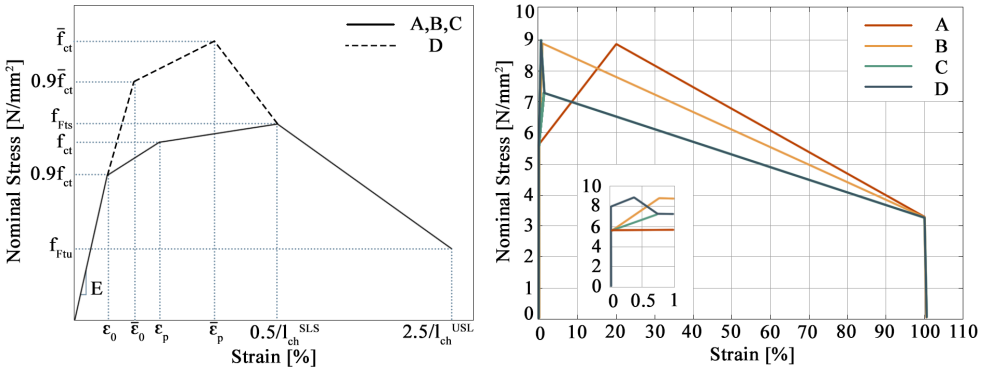

Fig. 7 Out-of-scale scheme of constitutive laws adopted in the four cases considered (left); nominal stress vs. strain curve of the four cases considered (right).

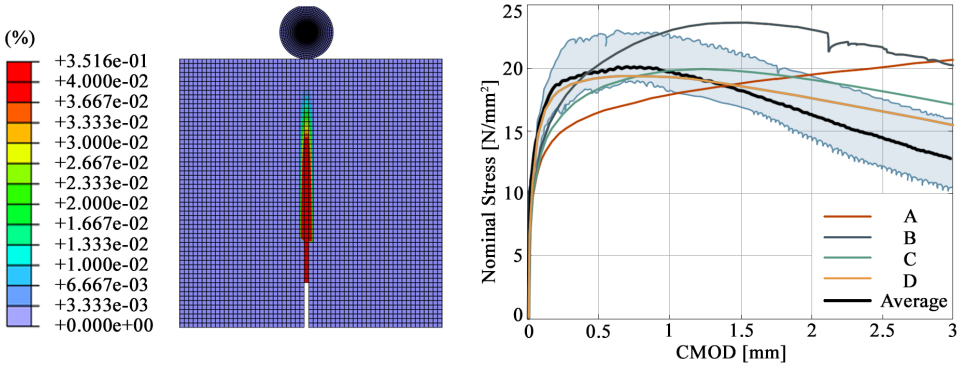

Fig. 8 Equivalent plastic strain in uniaxial tension (PEEQT) in the notched region at CMOD = 1.1 mm which corresponds to step h) in DIC measurements (left); Nominal stress vs. CMOD of the four cases considered compared to the average experimental curve (right).

5 Future developments

The work presented here is part of a wider experimental campaign to characterize the treated UHPFRC material. The forthcoming experimental campaign ranges from constitutive investigation to structural response also considering the roles of notch in mechanical characterization of UHPFRC materials. The results will allow the development of a more refine back calculation procedure for the definition of the uniaxial tensile law able to predict the structural response by numerical application. Table 4 shows the test program.

Table 4 Future experimental program.

Type of test	Specimen	Specimen size [mm]	N. of tests
3PB	beam (notch 25 mm)	150x150x600	6
3PB	beam (unnotched)	150x125x600	3
4PB	beam (notch 25 mm)	150x150x600	3
4PB	beam (unnotched)	150x125x600	3
4PB	beam (unnotched)	150x20x600	3
bending with center load	circular plate	Φ560 t20	3
direct tensile	dumbbell-shaped	L440 t20	6
direct tensile	cylinder (notched)	Φ60 h100	6

6 Conclusions

The paper discusses the reliability of commercial numerical models in predicting the flexural response of notched UHPFRC beams. The analysis results show a large variability depending on the choice of regularization length and tensile law shape. Based on the results discussed, the following conclusions can be drawn:

- to study the multicrack zone, the DIC technique is proposed. This method is able to capture the multicracks that are otherwise difficult to see by naked eye and by the traditional transducer;
- generally the uniaxial tensile constitutive law proposed by Model Code 2010 does not capture the actual shape of the experimental response. Moreover the selection of the characteristic length play a key role in assessing the reliability of the procedure.

- the results of the numerical modelling are more similar to the experimental curve if the formula $f_{Fts} = 0.37 \cdot f_{R1}$ is used;
- the results show the large importance of the correct definition of the pre-peak branch; this seems to univocally affect the prediction of the mechanical response for small CMODs.

References

[1] Naaman, Antoine E., and Hans-Wolf Reinhardt. 2006. "Proposed classification of HPFRC composites based on their tensile response." *Materials and structures* 39.5: 547-555.

[2] Kanakubo, Toshiyuki. 2006. "Tensile characteristics evaluation method for ductile fiber-reinforced cementitious composites." *Journal of Advanced Concrete Technology* 4.1: 3-17.

[3] Taerwe, Luc, and Stijn Matthys. 2013. "Fib Model Code for Concrete Structures 2010". *Ernst & Sohn, Wiley*.

[4] López, J. Á., Serna, P., Navarro-Gregori, J., and Coll, H. 2016. "A simplified five-point inverse analysis method to determine the tensile properties of UHPFRC from unnotched four-point bending tests." *Composites Part B: Engineering* 91: 189-204.

[5] EN 14651:2005. Test method for metallic fibered concrete - Measuring the flexural tensile strength (limit of proportionality (LOP), residual). Brussels: European Committee for Standardization.

[6] McCormick, Nick, and Jerry Lord. 2010. "Digital image correlation." *Materials today* 13.12: 52-54.

[7] Jones, E. M. C. 2015. Matlab-based DIC code - version 4, University of Illinois.

[8] Belletti, Beatrice, Cecilia Damoni, and Max AN Hendriks. 2011. "Development of guidelines for nonlinear finite element analyses of existing reinforced and pre-stressed beams." *European Journal of Environmental and Civil Engineering* 15.9: 1361-1384.

[9] Di Prisco, M., Colombo, M., and Dozio, D. 2013. Fibre-reinforced concrete in fib Model Code 2010: principles, models and test validation. *Structural Concrete*, 14(4), 342-361.